Mineralogical Magazine (2023), **87**, 731–737
doi:10.1180/mgm.2023.45

CAMBRIDGE UNIVERSITY PRESS

Article

Fluorbritholite-(Nd), $Ca_2Nd_3(SiO_4)_3F$, a new and key mineral for neodymium sequestration in REE skarns

Dan Holtstam[1], Patrick Casey[2], Luca Bindi[3], Hans-Jürgen Förster[4], Andreas Karlsson[1] and Oona Appelt[4]

[1]Department of Geosciences, Swedish Museum of Natural History, Box 50007, SE-104 05 Stockholm, Sweden; [2]Geological Survey of Sweden, Villavägen 18, SE-752 36, Uppsala, Sweden; [3]Dipartimento di Scienze della Terra, Università degli Studi di Firenze, Via G. La Pira 4, 50121, Firenze, Italy; and [4]Helmholtz Centre Potsdam GFZ German Research Centre for Geosciences, Telegrafenberg, 14473 Potsdam, Germany

Abstract

Fluorbritholite-(Nd), ideally $Ca_2Nd_3(SiO_4)_3F$, has been approved by the International Mineralogical Association (IMA2023–001) and constitutes a new member of the britholite group of the apatite supergroup. It occurs in skarn from the Malmkärra iron mine, Norberg, Västmanland (one of the Bastnäs-type deposits in Sweden), associated with calcite, dolomite, magnetite, lizardite, talc, fluorite, baryte, scheelite, gadolinite-(Nd) and other REE minerals. Fluorbritholite-(Nd) forms anhedral and small grains, rarely up to 250 μm across. They are brownish pink and transparent with a vitreous to greasy lustre. The mineral is brittle, with an uneven or subconchoidal fracture and lacks a cleavage. In thin section, the mineral is nonpleochroic, uniaxial (–). D_{calc} = 4.92(1) g·cm^{-3} and n_{calc} = 1.795. The empirical chemical formula from electron microprobe (WDS) point analyses is $(Ca_{1.62}Nd_{0.97}Ce_{0.83}Y_{0.52}Sm_{0.30}Gd_{0.23}Pr_{0.17}La_{0.16}Dy_{0.11}Er_{0.03}Tb_{0.03}Ho_{0.01}Yb_{0.01})_{\Sigma 4.99}(Si_{2.92}P_{0.08}As_{0.01})_{\Sigma 3.01}O_{12.00}[O_{0.48}F_{0.26}(OH)_{0.14}Cl_{0.10}Br_{0.02}]_{\Sigma 1.00}$. The crystal structure of fluorbritholite-(Nd) was refined from single-crystal X-ray diffraction data to R_1 = 0.043 for 704 unique reflections. It belongs to the hexagonal system, space group $P6_3/m$, with unit cell parameters a = 9.5994(3), c = 6.9892(4) Å and V = 557.76(5) Å^3 for Z = 2. Fluorbritholite-(Nd) and other britholite-group minerals are a major sink for neodymium in REE-bearing skarns of Bastnäs type.

Keywords: fluorbritholite-(Nd); britholite group; apatite supergroup; new mineral; crystal structure; neodymium; REE ore; skarn; Norberg; Sweden

(Received 21 April 2023; accepted 2 June 2023; Accepted Manuscript published online: 8 June 2023; Associate Editor: Daniel Atencio)

Introduction

The global quest for economic sources of rare earth elements (REE), prompted by the increased demand for neodymium (Nd) and related critical metals as components in e.g. permanent magnetic materials and lasers (Chakhmouradian and Wall, 2012; Goodenough *et al.*, 2018), has revived interest in REE deposits of the Bergslagen ore region in Sweden (Sadeghi *et al.*, 2019). In particular, the occurrences of skarn-hosted britholite-group minerals — referred to as Bastnäs-type deposits, subtype 2, by Holtstam and Andersson (2007) — in the Norberg District are of interest because of their unusual enrichment in heavier REE. Previous work (Holtstam and Andersson, 2007) included a few chemical analyses of britholite-group minerals suggesting the existence of a Nd-dominant species, corresponding to UM2007–044 in the list of valid unnamed mineral species (Smith and Nickel, 2007). It has now been approved by the Commission on New Minerals, Nomenclature and Classification of the International Mineralogical Association (IMA2023–001, Holtstam *et al.*, 2023) with the name fluorbritholite-(Nd), ideally $Ca_2Nd_3(SiO_4)_3F$. The mineral was discovered at one of the Bastnäs-type deposits, Malmkärra, during a recent survey and sampling campaign. Type material is preserved in the mineral collection of the Department of Geosciences, Swedish Museum of Natural History, Box 50007, SE-10405 Stockholm, Sweden, under collection number GEO-NRM #20220221 (specimen and polished section). The accepted mineral symbol for fluorbritholite-(Nd) is Fbri-Nd.

Occurrence

The Malmkärra iron mine is situated close to the tarn Stora Malmtjärnen, Norberg, Västmanland County, Sweden (60° 3′34″N, 15°50′45″E, 200 m a.s.l.). The deposit is hosted in a synclinal marble layer (dolomite), intercalated with felsic metavolcanic beds, and is divided into separate ore bodies due to local faulting (Geijer, 1936). The underlying bedrock consists of plastically deformed mica-schist, with major quartz, muscovite and cordierite, along with accessory tourmaline, magnetite and allanite-(Ce). It grades into a Na-rich, less altered metavolcanic rock in certain sections. The magnetite-skarn ore has locally replaced the carbonate along its contact with the country rock (Geijer, 1936; Holtstam *et al.*, 2014).

The oldest record of the Malmkärra mine is from 1664. Magnetite ore was mined (~100,000 t of Fe) until production stopped in 1936 (Geijer and Magnusson, 1944). Geijer (1927)

Corresponding author: Dan Holtstam; Email: dan.holtstam@nrm.se
Cite this article: Holtstam D., Casey P., Bindi L., Förster H.-J., Karlsson A. and Appelt O. (2023) Fluorbritholite-(Nd), $Ca_2Nd_3(SiO_4)_3F$, a new and key mineral for neodymium sequestration in REE skarns. *Mineralogical Magazine* **87**, 731–737. https://doi.org/10.1180/mgm.2023.45

Figure 1. Colour image of cut slab of boulder from Malmkärra, GEO-NRM #20220221. Dark spots are mostly serpentine, greyish areas carbonate. Fluorbritholite-(Nd) was obtained from the magnetite-rich part encircled.

first noted the REE mineralisation, later referred to as Bastnäs-type (Geijer, 1961). The mineralisation occurs as bands of REE-bearing silicates deposited between magnetite-rich, tremolite-bearing skarns and dolomitic marble, with patches of Mg silicates (humite and serpentine) in recrystallised carbonate rock ('ophicalcite'). Malmkärra is the type locality for three rare mineral species so far: västmanlandite-(Ce) (Holtstam *et al.*, 2005), ulfanderssonite-(Ce) (Holtstam *et al.*, 2017) and gadolinite-(Nd) (Škoda *et al.*, 2018). According to a recent estimation (Rönnåsen, 2023), there is still 83,000 t of waste rock present in the mine area, with an average of 0.55% REE.

Fluorbritholite-(Nd) was discovered in a boulder from the old dumps (Fig. 1). All observed occurrences of the new mineral relate to a thin skarn zone situated at the contact between the 'ophicalcite' and magnetite ore. Associated minerals in this skarn band include calcite, dolomite, magnetite, lizardite, talc, fluorite, baryte, scheelite and gadolinite-(Nd), accompanied by an allanite-group mineral and a gatelite-group mineral.

The Palaeoproterozoic (Orosirian) Bastnäs-type REE–Fe (± Cu, Bi, Mo, Co and Au) skarn mineralisations in the area originated from reactions involving hot ($T > 400$°C) magmatic–hydrothermal fluids containing REE–Si–chloro–fluoro ion complexes and primary carbonate (Holtstam and Broman, 2002; Holtstam *et al.*, 2014; Sahlström *et al.*, 2019).

Appearance and physical properties

Fluorbritholite-(Nd) has an irregular morphology, forming anhedral grains of small size (rarely up 250 μm across, Fig. 2). The colour is brownish pink, with a white streak. The crystals are transparent with a vitreous to greasy lustre. The hardness (Mohs) is estimated as 5, in analogy with fluorbritholite-(Ce). Fluorbritholite-(Nd) is brittle with an uneven or subconchoidal fracture. No parting or cleavage have been observed. Density was not measured because of the minute sample size; the calculated value is 4.92(1) g·cm^{-3}. In a petrographic thin section, the mineral is nonpleochroic and uniaxial (–). The refractive indices were not measured due to limited amount of type material

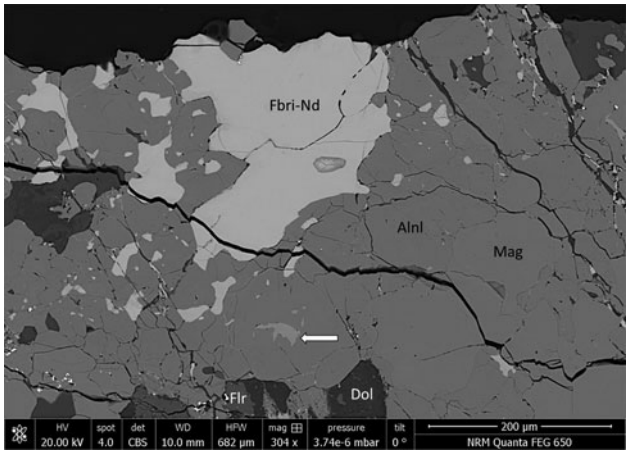

Figure 2. Back-scattered electron image of fluorbritholite-(Nd) (Fbri-Nd), an allanite-like mineral (Alnl), magnetite (Mag), fluorite (Flr) and dolomite (Dol). The white arrow points to a gatelite-like mineral. Sample GEO-NRM #20220221.

(only tiny fragments could be extracted from the one large grain in the type sample). Overall $n_{calc} = 1.795$ from Gladstone–Dale coefficients (Mandarino, 1981), very close to the highest available index liquid (1.80).

Chemical data

The chemical composition (Table 1) was determined using a JEOL JXA-8230 electron-microprobe operated in wavelength-dispersive mode (20 kV acceleration voltage, 10 nA sample current and 5 μm beam size). The number of spot analyses was 12. Natural and synthetic reference materials were used (Table 1). Measurements involved the following X-ray spectral lines and analysing crystals: Si and Al ($K\alpha$, TAP); Y and As ($L\alpha$, TAP); P, Ca and Cl ($K\alpha$, PETH); La, Ce and Lu ($L\alpha$, LIF); Gd and Tb ($L\beta$, LIF); Pr, Nd, Sm, Dy, Ho and Er ($L\beta$, LIFL); Yb ($L\alpha$, LIFL); F ($K\alpha$, LD1); Br ($K\alpha$, LIFL). Peak overlaps between various REE and F–Ce were corrected empirically. Thulium was not measured but calculated from chondrite normalisation. Iron, Ti, Al, Mg, U, Pb and Th were sought but found to be below the detection limit. The H_2O content was not measured directly because of the small sample volume; it was inferred from structural, chemical and spectroscopic data.

The empirical formula calculated on the basis of 8 cations can be written as: $(Ca_{1.62}Nd_{0.97}Ce_{0.83}Y_{0.52}Sm_{0.30}Gd_{0.23}Pr_{0.17}La_{0.16}Dy_{0.11}Er_{0.03}Tb_{0.03}Ho_{0.01}Yb_{0.01})_{\Sigma 4.99}(Si_{2.92}P_{0.08}As_{0.01})_{\Sigma 3.01}O_{12}[O_{0.48}F_{0.26}(OH)_{0.14}Cl_{0.10}Br_{0.02}]_{\Sigma 1.00}$ The ideal mineral formula is $Ca_2Nd_3(SiO_4)_3F$, which requires (in wt.%) CaO 13.88, Nd_2O_3 62.45, SiO_2 22.31, F 2.35, F ≡ O – 0.99, sum 100.00.

Raman spectroscopy

Micro-Raman measurements were conducted using a Horiba (Jobin Yvon) LabRam HR Evolution instrument on a randomly oriented crystal. The sample was excited with frequency-doubled 532 nm and 785 nm Nd–YAG lasers utilising an Olympus 100 × objective (numerical aperture = 0.9). The lateral resolution of the unpolarised confocal laser beam was in the order of 1 μm. Raman spectra of the sample were collected through two acquisition cycles with single counting times of 45 s. Spectra were generated in the range of 100 to 4000 cm^{-1} utilising a 600 grooves/cm

https://doi.org/10.1180/mgm.2023.45 Published online by Cambridge University Press

Table 1. Chemical data (in wt.%) for fluorbritholite-(Nd).

Constituent	Mean	Range	2σ	Reference material
P_2O_5	0.68	0.60–0.78	0.14	$CePO_4$
As_2O_5	0.08	0.00–0.14	0.08	cobaltite
SiO_2	21.03	20.60–21.26	0.45	wollastonite
Y_2O_3	7.01	6.78–7.39	0.40	YPO_4
La_2O_3	3.23	2.90–3.45	0.36	$LaPO_4$
Ce_2O_3	16.35	15.43–17.20	1.10	$CePO_4$
Pr_2O_3	3.31	3.12–3.46	0.22	$PrPO_4$
Nd_2O_3	19.51	19.19–19.84	0.42	$NdPO_4$
Sm_2O_3	6.34	5.93–6.66	0.39	$SmPO_4$
Gd_2O_3	4.95	4.65–5.46	0.49	$GdPO_4$
Tb_2O_3	0.56	0.46–0.66	0.13	$TbPO_4$
Dy_2O_3	2.52	2.33–2.76	0.28	$DyPO_4$
Ho_2O_3	0.32	0.27–0.43	0.08	$HoPO_4$
Er_2O_3	0.67	0.56–0.75	0.10	$ErPO_4$
Tm_2O_3*	0.07	0.06–0.09	0.02	
Yb_2O_3	0.31	0.27–0.39	0.06	$YbPO_4$
Lu_2O_3	0.03	0.01–0.04	0.02	$LuPO_4$
CaO	10.86	10.65–11.07	0.29	apatite
H_2O**	0.15			
F	0.60	0.49–0.70	0.14	fluorite
Cl	0.42	0.39–0.45	0.04	tugtupite
Br	0.17	0.00–0.47	0.33	bromargyrite
F = O	−0.25			
Cl = O	−0.09			
Br = O	−0.02			
Total	98.81			

*Calculated value from chondrite normalisation ** H_2O calculated on the basis of (OH + F + Cl + Br + O) = 13 apfu.

grating and a thermoelectric-cooled charge-coupled device (CCD). The wavenumber calibration was performed using the 520.7 cm^{-1} Raman band on a polished silicon wafer with a wavenumber accuracy usually better than 0.5 cm^{-1}.

The spectra are largely overwhelmed by fluorescence. There is a distinct peak at 852 cm^{-1} in the 532 nm spectrum (Fig. 3), resulting from symmetric stretching of SiO_4 groups, and a weak one at 950 cm^{-1} corresponding to a contribution from the minor PO_4 group (ν_1 symmetric stretching; cf. Boughzala *et al.*, 2008). A sample of P-rich fluorbritholite-(Ce) from Norra Kärr, Sweden, has bands close to these positions (RRUFF no. R070412). A weak signal at 3300–3400 cm^{-1} in the 785 nm spectrum (Fig. 4) can be related to O–H stretching vibration modes.

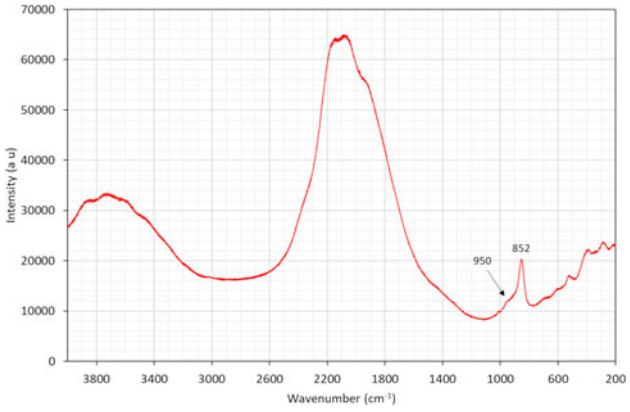

Figure 3. Raman spectrum of fluorbritholite-(Nd), obtained with a 532 nm laser.

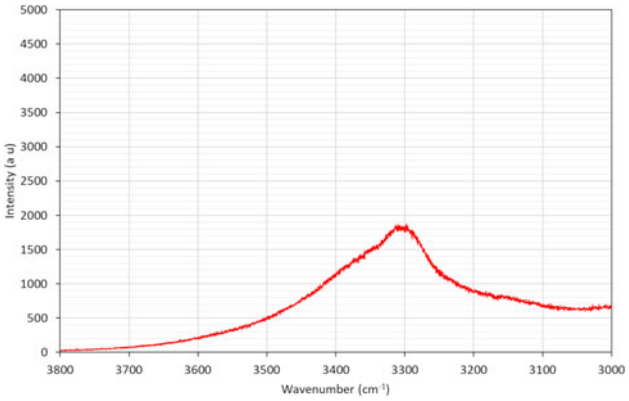

Figure 4. Raman spectrum of fluorbritholite-(Nd), obtained with a 785 nm laser.

X-ray crystallography

Single-crystal X-ray diffraction

Single-crystal X-ray diffraction data were collected with a Bruker D8 Advance from a 0.060 × 0.055 × 0.045 mm fragment, extracted from the largest available grain previously analysed with the electron microprobe (Fig. 1). The crystal structure of fluorbritholite-(Nd) was refined using *SHELXL-2013* (Sheldrick, 2008) starting from the atom coordinates of fluorbritholite-(Y) (Pekov *et al.*, 2011) to $R_1 = 0.043$ for 704 unique reflections. Crystal parameters and refinement conditions are given in Table 2. Refined atom coordinates, site occupancies and equivalent isotropic displacement parameters are reported in Table 3. Selected interatomic distances are provided in Table 4. The bond valence sums (site populations given in the notes to the

Table 2. Single-crystal data and experimental details.

Crystal data	
Ideal formula	$Ca_2Nd_3(SiO_4)_3F$
Crystal system	Hexagonal
Space group	$P6_3/m$
a (Å)	9.5994(3)
c (Å)	6.9892(4)
V (Å^3)	557.76(5)
Z	2
Data collection	
Diffractometer	Bruker D8 Advance
Distance to detector (cm)	5
Scan modes	ω
Exposure time per frame (s)	25
Radiation type	Mo*K*α (λ = 0.71073 Å)
Temperature (K)	293
Collected reflections	14017
Unique reflections	704
Reflections with $F_o > 4\sigma(F_o)$	578
2θ range (°)	2.45–32.04
R_{int}	0.071
Refinement	
Refinement	Full-matrix least square on F^2
No. of least-square parameters	42
Final R_1 [$F_o > 4\sigma(F_o)$]	0.043
Final R_1	0.055
Final wR^2 [$F_o > 4\sigma(F_o)$]	0.100
Final wR^2	0.108
GooF	1.102
$\Delta\rho_{max}$, $\Delta\rho_{min}$ ($e^- \times$ Å^{-3})	3.03, −3.29

Note: $wR^2 = [\Sigma\ w\ (|F_o|^2 - |F_c|^2)^2\ /\ \Sigma\ w\ (|F_o|^4)]^{½}$.

https://doi.org/10.1180/mgm.2023.45 Published online by Cambridge University Press

Table 3. Refined fractional atom coordinates, equivalent displacement parameters (Å^2) and site occupancies in fluorbritholite-(Nd).

Site	Site occupancy	*x*	*y*	*z*	U_{eq}
*M*1	$La_{0.658(13)}Ca_{0.342(13)}$	0.3333	0.6667	0.00045(13)	0.0237(3)
*M*2	$La_{0.705(13)}Ca_{0.295(13)}$	0.24039(9)	0.99206(9)	¼	0.0265(3)
Si	$Si_{1.00}$	0.4017(3)	0.3730(3)	¼	0.0206(7)
O2	$O_{1.00}$	0.3268(11)	0.4899(10)	¼	0.0339(18)
O3	$O_{1.00}$	0.5962(9)	0.4683(9)	¼	0.037(2)
O4	$O_{1.00}$	0.3461(11)	0.2556(8)	0.0643(10)	0.052(2)
O1	$O_{0.81}$	0.0000	0.0000	¼	0.081(12)
Cl1	$Cl_{0.095}$	0.0000	0.0000	0.093(13)	0.081(12)

table), computed with the parameters given by Brese and O'Keeffe (1991), are listed in Table 5. Considering the correspondence in atomic number ('mean' atomic number of [REE + Y] = 56.8 in fluorbritholite-(Nd)), we used La (atomic number = 57) as the average REE in the refinement. The crystallographic information file has been deposited with the Principal Editor of Mineralogical Magazine and is available as Supplementary material (see below).

Powder X-ray diffraction

Powder X-ray diffraction data (Table 6) were collected with an Oxford Diffraction Excalibur PX Ultra diffractometer fitted with a 165 mm diagonal Onyx CCD detector and using copper radiation (Cu*Kα*, λ = 1.54138 Å) from the same crystal used for the single-crystal experiment. The hexagonal $P6_3/m$ unit-cell parameters refined from powder data are $a = 9.5966(7)$ Å, $c = 6.9816(8)$ Å and $V = 556.83(7)$ Å^3.

Results and discussion

Crystal structure

Fluorbritholite-(Nd) has the hexagonal $P6_3/m$ apatite-type structure, with the general formula $M1_2M2_3(TO_4)_3X$, in this case based on *T* = Si plus minor P at the tetrahedrally coordinated sites and polyhedra of $M1O_9$ and $M2O_6X$ (*M* = Ca and REE; *X* = O, F, OH and Cl). Calcium and the REE are essentially disordered over the *M* sites. The slight preponderance of REE at *M*2 agrees with the pattern seen in previously studied LREE-rich fluorbritholite-(Ce) (Oberti *et al.*, 2001; Zubkova *et al.*, 2015), where this preference is even more pronounced. The *X* anions are in channels parallel to the 6-fold axis. The *X* site is split; whereas the smaller anions lie on the mirror plane at *z* = ¼ and Cl is found at distance of 1.1 Å below or above. The site occupancy of the two split sites was fixed during the refinement according to the compositional data obtained from microprobe analyses. The bond valence sums are in good agreement with the site populations and conformable with all lanthanides being trivalent (the presence of tetravalent Ce is highly unlikely as the mineral was deposited in a magnetite-bearing skarn). No symmetry lowering was observed for this sample (cf. Oberti *et al.*, 2001).

Table 4. Selected interatomic distances (Å) in fluorbritholite-(Nd).*

*M*1–O2	2.412(5) ×3	*M*2–O1	2.3466(8)
*M*1–O3	2.465(6) ×3	*M*2–O4	2.365(6) ×2
*M*1–O4	2.816(9) ×3	*M*2–O3	2.424(8)
		*M*2–O4'	2.558(7) ×2
Si–O2	1.608(8)	*M*2–Cl1	2.59(4) ×2
Si–O3	1.617(8)	*M*2–O2	2.765(10)
Si–O4	1.624(6) ×2		

*The O1/Cl1 positions, giving rise to the 7-fold coordinated *M*2 polyhedron, are mutually present.

Table 5. Bond valence sums (BVS) for fluorbritholite-(Nd) calculated with the parameters of Brese and O'Keeffe (1991).*

	*M*1	*M*2	Si	ΣO
O1 (81%)		$0.442^{\times3\rightarrow}$		1.33
O2	$0.390^{\times3\downarrow\times2\rightarrow}$	0.153	1.047	1.98
O3	$0.337^{\times3\downarrow\times2\rightarrow}$	0.383	1.023	2.08
O4	$0.130^{\times3\downarrow\times2\rightarrow}$	$0.450^{\times2\downarrow}$ $0.267^{\times2\downarrow}$	$1.003^{\times2\downarrow}$	1.98
Cl1 (19%)		$0.131^{\times2\downarrow\times3\rightarrow}$		0.39
BVS	2.57	2.67	4.08	

*$M1 = REE_{0.66}Ca_{0.34}$; $M2 = REE_{0.70}Ca_{0.30}$, with REE = $Nd_{0.31}Ce_{0.26}Y_{0.16}Sm_{0.10}Gd_{0.07}Pr_{0.05}La_{0.05}$

Remarks on nomenclature

The type specimen of fluorbritholite-(Nd) has a surplus of ΣREE atoms (> 3 atoms per formula unit) relative the ideal formula, which must be charge-compensated by introducing a significant REE oxysilicate apatite ($CaLn_4[SiO_4]_3O$) component (e.g.

Table 6. Observed and calculated X-ray powder diffraction data (*d* in Å) for fluorbritholite-(Nd).*

	Observed		Calculated	
hkl	d_{obs}	I_{est}	d_{calc}	I_{calc}
110			4.7997	4
200	4.16	20	4.1567	27
111			3.9566	19
002			3.4946	14
102	**3.223**	**30**	3.2215	31
120	**3.144**	**30**	3.1421	32
121	**2.866**	**100**	2.8658	100
112	**2.823**	**55**	2.8251	62
300	**2.769**	**35**	2.7711	44
202			2.6749	5
130			2.3057	6
302			2.1713	4
113			2.0959	10
400			2.0783	4
222	**1.977**	**40**	1.9783	31
132			1.9245	16
230			1.9072	4
123	1.869	25	1.8714	29
231			1.8399	18
140			1.8141	19
402	1.785	25	1.7863	24
004			1.7473	12
240			1.5711	3
331			1.5596	6
124			1.5271	8
502			1.5014	9
304			1.4780	8
323			1.4758	5
511			1.4602	4
332			1.4547	6
215			1.2772	3
414			1.2585	10
252			1.2440	6
440			1.1999	4
116			1.1320	3

*The calculated diffraction pattern is obtained with the atom coordinates reported and the site occupancies given in Table 3 (only reflections with $I_{rel} \geq 3$ are listed); the strongest observed Bragg reflections are given in bold.

https://doi.org/10.1180/mgm.2023.45 Published online by Cambridge University Press

Kobayashi and Sakka, 2014). A similar component was in part inferred for fluorbritholite-(Y) (Pekov *et al.*, 2011). However, as the sum of monovalent *X* atoms exceeds the amount of O^{2-}, the name prefix is decided by the dominating F (see Pasero *et al.*, 2010), in accord with the dominant-valency rule (Hatert and Burke, 2008). The small Br concentration varies to some extent within the grain and is essentially antipathetic to Cl (linear correlation coefficient $R^2 = -0.33$), but is not correlated with any other element. It is thus ascertained that the sum of monovalent ions is > 0.5 apfu in this crystal. Fluorbritholite-(Nd) is a member of the britholite group of the apatite supergroup (Pasero *et al.*, 2010). It represents the Nd-analogue of fluorbritholite-(Ce) and fluorbritholite-(Y) (Table 7), and belongs to the Strunz group 9.AH.25 (Strunz and Nickel, 2001).

Geochemical considerations

In the present mineral assemblage, the allanite-like mineral, with large Ce, La, Mg and Fe^{3+} contents but no measurable F, represents the dominant REE mineral. REE-fluorocarbonates (e.g. bastnäsite) are notably absent, but quite common elsewhere in the REE skarn. As it appears from the chondrite-normalised patterns of the two major REE minerals and a bulk sample from Malmkärra, fluorbritholite-(Nd) is a major sink for Nd in the skarn system (Fig. 5). Similar, nearly flat REE profiles also prevail for gadolinite-subgroup minerals (Škoda *et al.*, 2018), arrheniusite-(Ce) (Holtstam *et al.*, 2021) and magnesiorowlandite-(Y) (Holtstam and Andersson, 2007), but these minerals occur in much less quantities in the deposits of the Norberg District. In fact, all fluorbritholite samples here (Fig. 6) contain significant Nd (11.5–19.8 wt.% Nd_2O_3; Holtstam and Andersson, 2007, and this work), with a generally antipathetic relation between Ce and Y (12.8–31.7% Ce_2O_3 vs. 13.9–0.9% Y_2O_3). In the Nya Bastnäs deposit (belonging to sub-type 1 in the terminology of Holtstam and Andersson, 2007), the cerite-group minerals are similarly enriched in Nd, however no Nd-dominant member has been found to date.

Compared to the chemical fingerprint of britholite-group minerals, which are predominantly of magmatic–volcanic origin (Della Ventura *et al.*, 1999; Zozulya *et al.*, 2015; Zubkova *et al.*, 2015; Zozulya *et al.*, 2017; Lorentz *et al.*, 2019), the Norberg samples are poor in Ca, despite crystallisation in a carbonate-rich

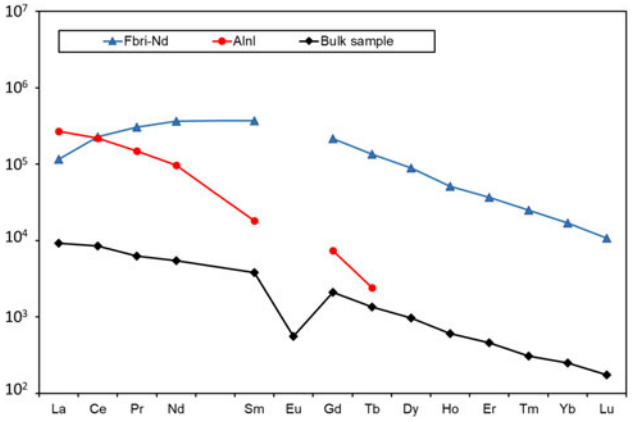

Figure 5. Chondrite-normalised REE patterns for fluorbritholite-(Nd) (Fbri-Nd), the coexisting allanite-like mineral (Alnl) and the bulk system (obtained with lithium borate fusion and ICP-MS) at Malmkärra. Chondrite values were taken from Boynton (1984).

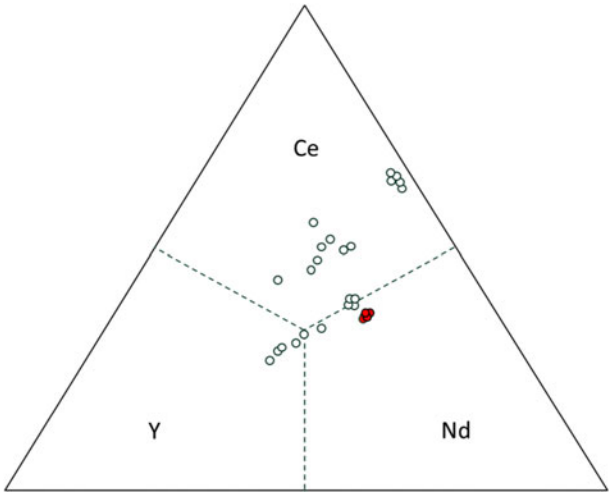

Figure 6. Triangular plot of Ce:Nd:Y atomic ratios in fluorbritholite samples from the Norberg area, Västmanland, Sweden. Filled circles correspond to the analyses of fluorbritholite-(Nd) from this study. Open symbols refer to data reported by Holtstam and Andersson (2007).

Table 7. Comparison of fluorbritholite species.

	Fluorbritholite-(Nd)	Fluorbritholite-(Ce)	Fluorbritholite-(Y)
Ideal IMA formula	$Ca_2Nd_3(SiO_4)_3F$	$(Ce,Ca)_5(SiO_4)_3F$	$(Y,Ca)_5(SiO_4)_3F$
Ideal advised formula	$Ca_2Nd_3(SiO_4)_3F$	$Ca_2Ce_3(SiO_4)_3F$	$Ca_2Y_3(SiO_4)_3F$
Space group	$P6_3/m$	$P6_3/m$	$P6_3/m$
Unit-cell parameters	a = 9.5994(3) Å	a = 9.517 Å	a = 9.4437(2) Å
	c = 6.9892(4) Å	b = 6.983 Å	c = 6.8169 (2) Å
	V = 557.76(5) Å^3	V = 547.7 Å^3	V = 526.50(2) Å^3
	Z = 2	Z = 2	Z = 2
Strongest Bragg	4.16 (20)		4.10 (27)
peaks, Å (%)	3.22 (30)		3.16 (27)
	3.144 (30)		3.102 (29)
	2.866 (100)	2.845 (100)	2.826 (100)
	2.823 (55)	2.822 (40)	2.775 (58)
	2.769 (35)	2.747 (30)	2.737 (46)
	1.977 (40)	1.970 (30)	1.948 (25)
Colour	pink to brownish	pale yellow – reddish brown	light pinkish–brown to dark brown
D_{calc} (g/cm^3)	4.91	4.66	4.61
Reference	This paper	Gu *et al.* (1994)	Pekov *et al.* (2011)

https://doi.org/10.1180/mgm.2023.45 Published online by Cambridge University Press

environment (dolomite). The apatite-type substitution, $Ca^{2+} + P^{5+} \leftrightarrow REE^{3+} + Si^{4+}$, is accordingly modest. Interestingly, the Ca-poor britholite samples of the skarn-related Anadol REE ores of the eastern Azov region, Ukraine (Khomenko *et al.*, 2013), are Nd-rich as well (up to 14 wt.% Nd_2O_3). The Norberg britholite-group minerals are also practically devoid of the actinides (<0.05 wt.%), which is exceptional. Exploitation of skarn-hosted REE deposits of this type is thus more environmentally friendly (owing to the toxicity and radiation protection aspects related to U and Th) and economically attractive, provided that larger tonnages can be secured.

Supplementary material. The supplementary material for this article can be found at https://doi.org/10.1180/mgm.2023.45.

Acknowledgements. We thank Matthias Konrad-Schmolke at the Univ. of Gothenburg for providing access to the Raman spectroscopy facility. Sample collection and preliminary analyses were conducted in the course of the governmental directive "Increasing the opportunities for sustainable extraction and recycling of minerals from secondary resources" by the Geological Survey of Sweden. We appreciate the constructive comments and suggestions by two anonymous reviewers and Structures Editor Peter Leverett.

Competing interest. The authors declare none.

References

Boughzala K., Salem E.B., Kooli F., Gravereau P. and Bouzouita K. (2008) Spectroscopic studies and Rietveld refinement of strontium-britholites. *Journal of Rare Earths*, **26**, 483–489.

Boynton W.V. (1984) Cosmochemistry of the rare earth elements: meteorite studies. Pp. 63–114 in: *Developments in Geochemistry* (P. Henderson, editor). Elsevier, Amsterdam.

Brese N.E. and O'Keeffe M. (1991) Bond-valence parameters for solids. *Acta Crystallographica*, **B47**, 192–197.

Chakhmouradian A.R. and Wall F. (2012) Rare earth elements: minerals, mines, magnets (and more). *Elements*, **8**, 333–340.

Della Ventura G., Williams C.T., Cabella R., Oberti R., Caprilli E. and Bellatreccia F. (1999) Britholite–hellandite intergrowths and associated REE-minerals from the alkali-syenitic ejecta of the Vico volcanic complex (Latium, Italy); petrological implications bearing on REE mobility in volcanic systems. *European Journal of Mineralogy*, **11**, 843–854.

Geijer P. (1927) Some mineral associations from the Norberg district. *Sveriges Geologiska Undersökning*, **C343**, 1–32.

Geijer P. (1936) Norbergs berggrund och malmfyndigheter. *Sveriges Geologiska Undersökning*, **Ca24**, 1–162.

Geijer P. (1961) The geological significance of the cerium mineral occurrences of the Bastnäs type in central Sweden. *Arkiv för Mineralogi och Geologi*, **3**, 99–105.

Geijer P. and Magnusson N.H. (1944) De mellansvenska järnmalmernas geologi. *Sveriges Geologiska Undersökning*, **Ca35**, 1–654.

Goodenough K.M., Wall F. and Merriman D. (2018) The rare earth elements: demand, global resources, and challenges for resourcing future generations. *Natural Resources Research*, **27**, 201–216.

Gu J., Tang S. and Chao G.Y. (1994) A new mineral – fluorbritholite-(Ce). *Journal of Wuhan University of Technology*, **9**, 9–14.

Hatert F. and Burke E.A.J. (2008) The IMA–CNMNC dominant-constituent rule revisited and extended. *The Canadian Mineralogist*, **46**, 717–728.

Holtstam D. and Andersson U.B. (2007) The REE minerals of the Bastnäs-type deposits, South-Central Sweden. *The Canadian Mineralogist*, **45**, 1073–1114.

Holtstam D. and Broman C. (2002) Lanthanide mineralizations of Bastnäs type: overview and new data. *GFF*, **124**, 230–231.

Holtstam D., Kolitsch U. and Andersson U.B. (2005) Västmanlandite-(Ce)-a new lanthanide-and F-bearing sorosilicate mineral from Västmanland, Sweden description, crystal structure, and relation to gatelite-(Ce). *European Journal of Mineralogy*, **17**, 129–141.

Holtstam D., Andersson U.B., Broman C. and Mansfeld J. (2014) Origin of REE mineralization in the Bastnäs-type Fe–REE–(Cu–Mo–Bi–Au) deposits, Bergslagen, Sweden. *Mineralium Deposita*, **49**, 933–966.

Holtstam D., Bindi L., Hålenius U., Kolitsch U. and Mansfeld J. (2017) Ulfanderssonite-(Ce), a new Cl-bearing REE silicate mineral species from the Malmkärra mine, Norberg, Sweden. *European Journal of Mineralogy*, **29**, 1015–1026.

Holtstam D., Bindi L., Bonazzi P., Förster H.J. and Andersson U.B. (2021) Arrheniusite-(Ce), $CaMg[(Ce_7Y_3)Ca_5](SiO_4)_3(Si_3B_3O_{18})(AsO_4)(BO_3)F_{11}$, a new member of the vicanite group, from the Östanmossa Mine, Norberg, Sweden. *The Canadian Mineralogist*, **59**, 177–189.

Holtstam D., Casey P., Bindi L., Förster H.-J. and Karlsson A. (2023) Fluorbritholite-(Nd), IMA 2023-001. CNMNC Newsletter 73. *Mineralogical Magazine*, **87**, https://doi.org/10.1180/mgm.2023.44.

Khomenko V.M., Rhede D., Kosorukov O.O. and Strekozov S.M. (2013) Britholite, cerite and bastnäsite in the Anadol ore occurrence (Eastern Azov area). *Mineralogical Journal* (*Ukraine*), **35**, 11–26.

Kobayashi K. and Sakka Y. (2014) Rudimental research progress of rare-earth silicate oxyapatites: their identification as a new compound until discovery of their oxygen ion conductivity. *Journal of the Ceramic Society of Japan*, **122**, 649–663.

Lorenz M., Altenberger U., Trumbull R.B., Lira R., de Luchi M.L., Günter C. and Eidner S. (2019) Chemical and textural relations of britholite- and apatite-group minerals from hydrothermal REE mineralization at the Rodeo de los Molles deposit, Central Argentina. *American Mineralogist*, **104**, 1840–1850.

Mandarino J.A. (1981) The Gladstone-Dale relationship; Part IV, The compatibility concept and its application. *The Canadian Mineralogist*, **19**, 441–450.

Oberti R., Ottolini L., Ventura G.D. and Parodi G.C. (2001) On the symmetry and crystal chemistry of britholite: New structural and microanalytical data. *American Mineralogist*, **86**, 1066–1075.

Pasero M., Kampf A.R., Ferraris C., Pekov I.V., Rakovan J. and White T.J. (2010) Nomenclature of the apatite supergroup minerals. *European Journal of Mineralogy*, **22**, 163–179.

Pekov I.V., Zubkova N.V., Chukanov N.V., Husdal T.A., Zadov A.E. and Pushcharovsky, D.Y. (2011) Fluorbritholite-(Y), $(Y,Ca,Ln)_5[(Si,P)O_4]_3F$, a new mineral of the britholite group. *Neues Jahrbuch für Mineralogie Abhandlungen*, **2011**, 191–197.

Rönnåsen L. (editor) (2023) *Hållbar utvinning och återvinning av metaller och mineral från sekundära resurser*. Sveriges Geologiska Undersökning, rapport 2023:1, Uppsala, Sweden, 137 pp.

Sadeghi M., Arvanitidis N., Ripa M., Jonsson E., Nysten P., Bergman T., Söderhielm J. and Claeson D. (2019) Rare earth elements distribution, mineralisation and exploration potential in Sweden. *Sveriges Geologiska Undersökning, Rapporter och meddelanden*, **146**, 1–184.

Sahlström F., Jonsson E., Högdahl K., Troll V.R., Harris C., Jolis E.M. and Weis F. (2019) Interaction between high-temperature magmatic fluids and limestone explains 'Bastnäs-type' REE deposits in central Sweden. *Scientific Reports*, **9**, 1–9.

Sheldrick G.M. (2008) A short history of SHELX. *Acta Crystallographica*, **A64**, 112–122.

Škoda R., Plášil J., Čopjaková R., Novák M., Jonsson E., Galiová M.V. and Holtstam D. (2018) Gadolinite-(Nd), a new member of the gadolinite supergroup from Fe–REE deposits of Bastnäs-type, Sweden. *Mineralogical Magazine*, **82**(S1), S133–S145.

Smith D.G.W. and Nickel E.H. (2007) A system of codification for unnamed minerals: Report of the subcommittee for unnamed minerals of the IMA Commission on New Minerals, Nomenclature and Classification. *The Canadian Mineralogist*, **45**, 983–1055.

Strunz H. and Nickel E.H. (2001) *Strunz Mineralogical Tables*, Ninth Edition. Schweizerbart'sche Verlagsbuchhandlung, Stuttgart, Germany, 870 pp.

Zozulya D.R., Lyalina, L.M. and Savchenko Y.E. (2015) Britholite ores of the Sakharjok Zr–Y–REE deposit, Kola Peninsula: Geochemistry, mineralogy, and formation stages. *Geochemistry International*, **53**, 892–902.

Zozulya D.R., Lyalina L.M. and Savchenko, Y.E. (2017) Britholite-group minerals as sensitive indicators of changing fluid composition during pegmatite formation: evidence from the Keivy alkaline province, Kola Peninsula, NW Russia. *Mineralogy and Petrology*, **111**, 511–522.

Zubkova N.V., Chukanov N.V., Pekov, I.V., Schäfer C., Yapaskurt V.O. and Pushcharovsky D.Y. (2015) Lanthanum-rich fluorbritholite-(Ce) from young alkaline volcanic rock of Eifel (Germany) and its crystal structure. Cation ordering in britholites. *Doklady Earth Sciences*, **464**, 936–939.

https://doi.org/10.1180/mgm.2023.45 Published online by Cambridge University Press